

Supporting Information

Hydrogel-based 3D fabrication of multiple replicas with varying sizes and materials from a single template via iterative shrinking

Eunseok Heo,^{‡a} Hye Been Koo,^{‡a} Jun Chang Yang,^a In Cho,^a Hyun-Hee Lee,^a Yong-Jin Yoon,^b Steve Park^a and Jae-Byum Chang^{*a,c}

^a Department of Materials Science and Engineering, Korea Advanced Institute of Science and Technology (KAIST), Daejeon 34141, Republic of Korea

^b Department of Mechanical Engineering, Korea Advanced Institute of Science and Technology (KAIST), Daejeon 34141, Republic of Korea

^c Department of Biological Sciences, Korea Advanced Institute of Science and Technology (KAIST), Daejeon 34141, Republic of Korea

*E-mail address: jbchang03@kaist.ac.kr

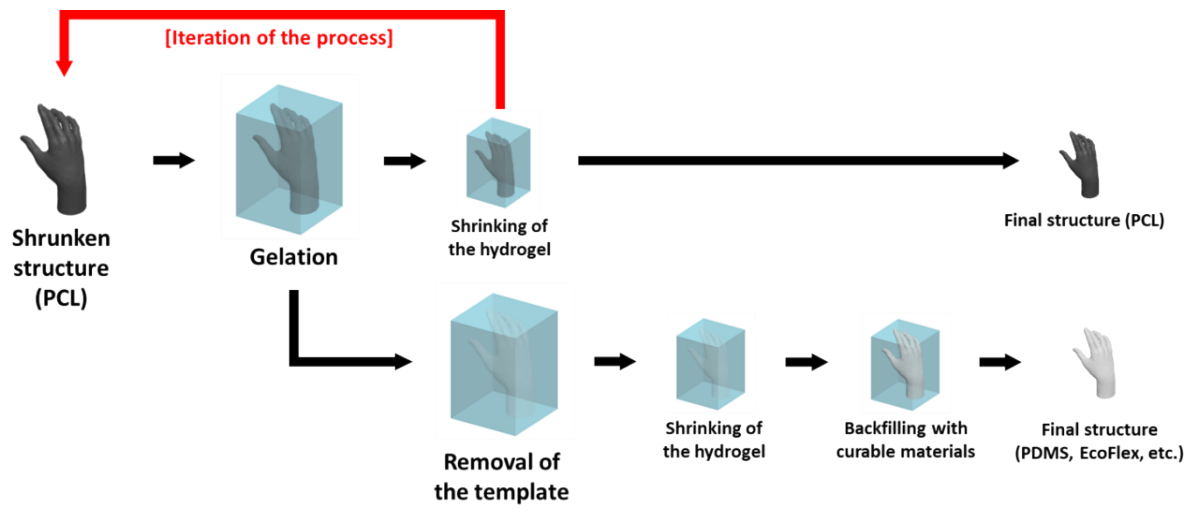


Fig. S1 Schematic illustration of the shrinking process after the second round.

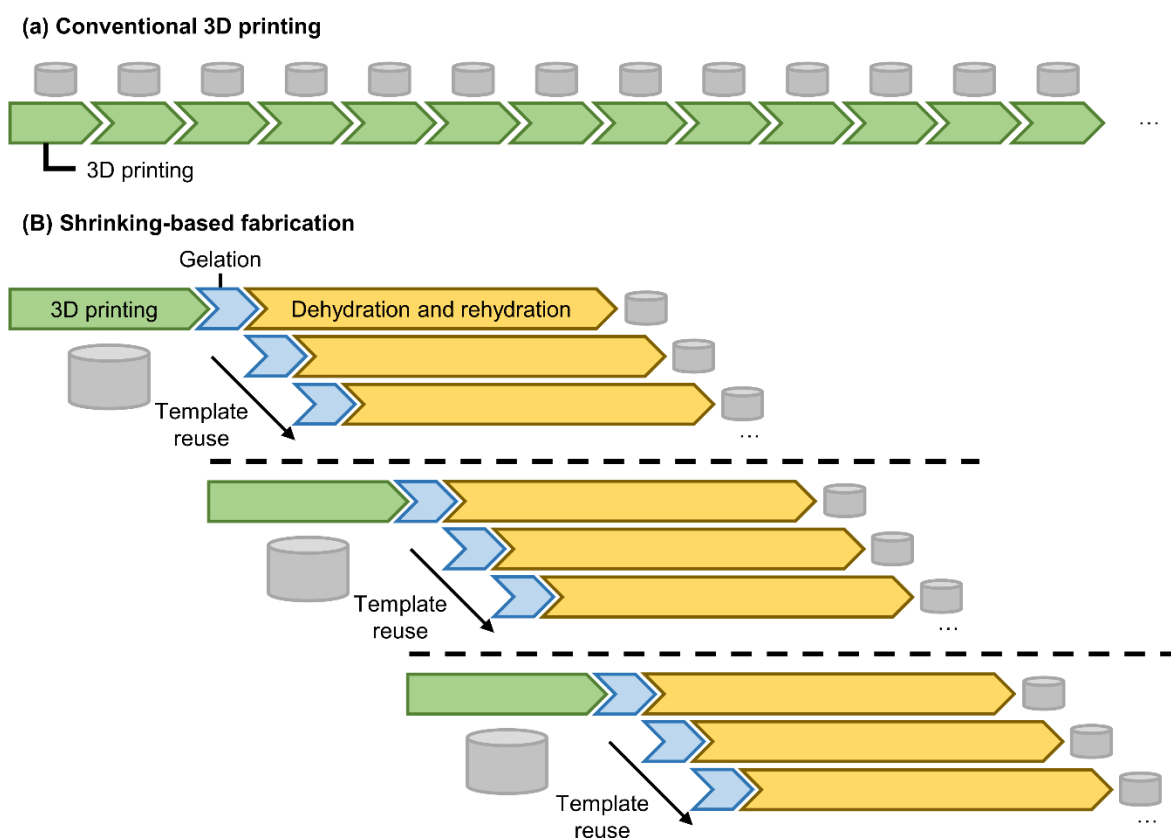


Fig. S2 Comparison between (a) conventional 3D printing, which requires printing separate structures for each size, and (b) the shrinking-based fabrication method, which allows the reuse of a single 3D-printed template to produce structures of various sizes through dehydration and rehydration cycles.

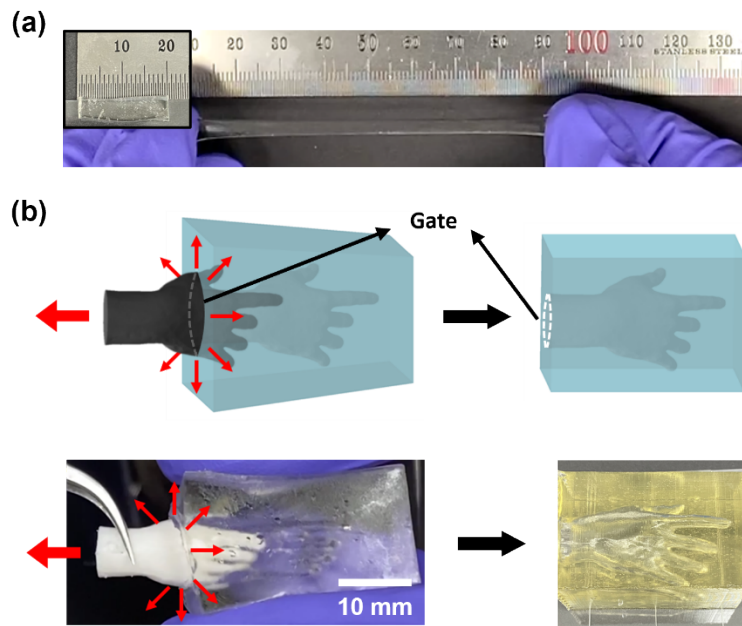


Fig. S3 (a) Images of the stretchable hydrogel before and after stretching. (b) Schematic illustration and images of 3D-printed template removal process using the stretchability of the hydrogel.

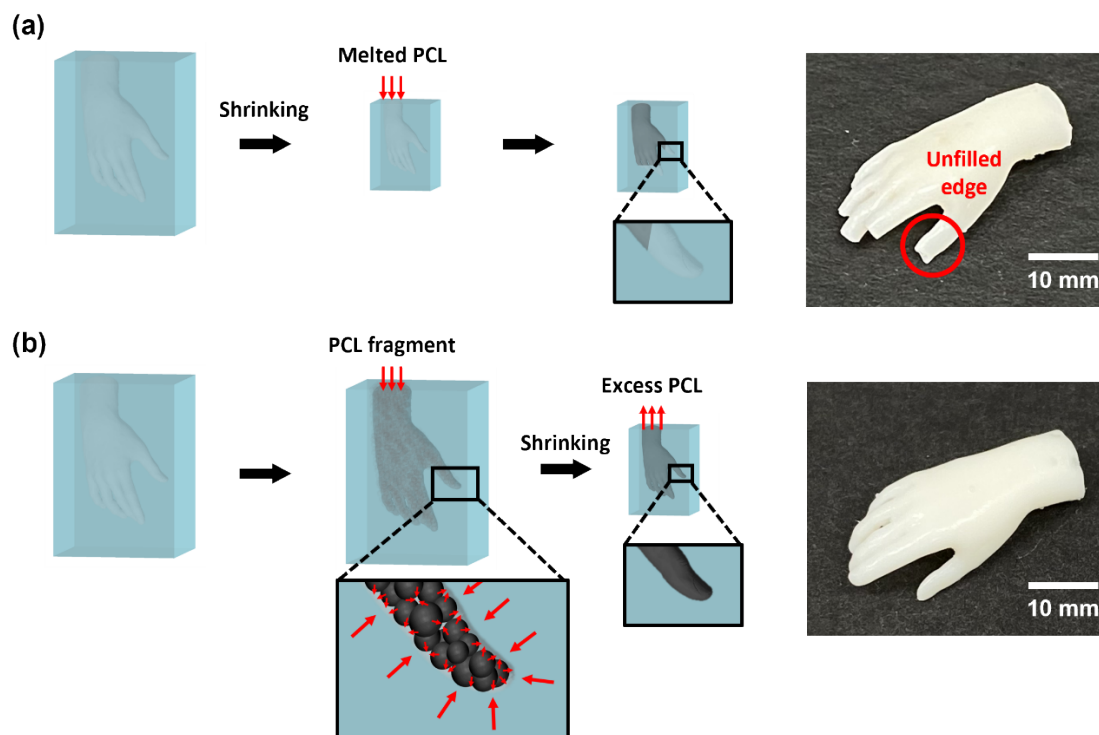


Fig. S4 Two processes of filling the hydrogel cavities with PCL: (a) removal of the template, shrinking of the hydrogel, and filling melted PCL, and (b) removal of the template, filling PCL fragments, and the shrinking of the hydrogel.

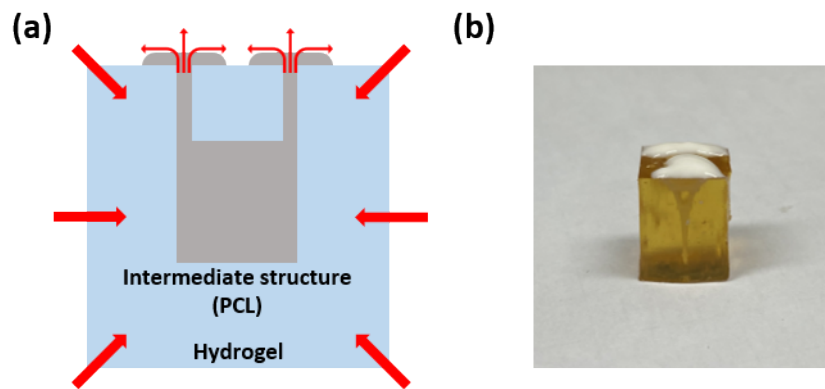


Fig. S5 (a) Schematic illustration of the shrinking of a hydrogel containing PCL. (b) Image of excess PCL being squeezed out by the pressure applied by the shrinking hydrogel.

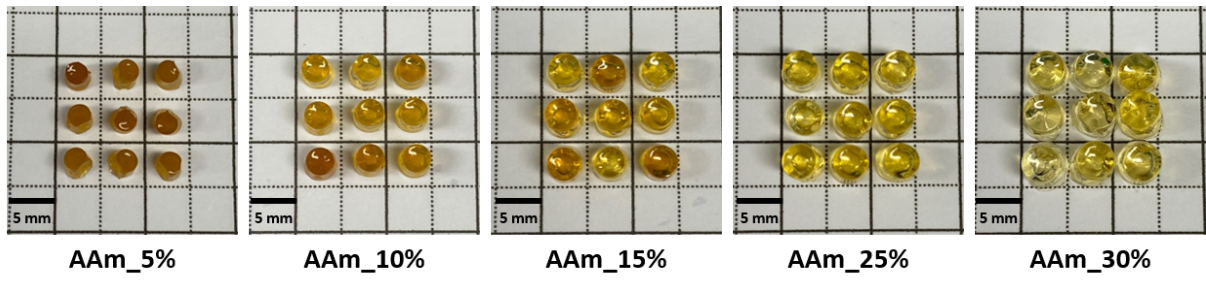


Fig. S6 Shrunken cylindrical hydrogels with AAm concentrations ranging from 5 wt% to 25 wt% in increments of 5 wt%, synthesized to analyze the shrinkage ratio. Scale bars are 5 mm.

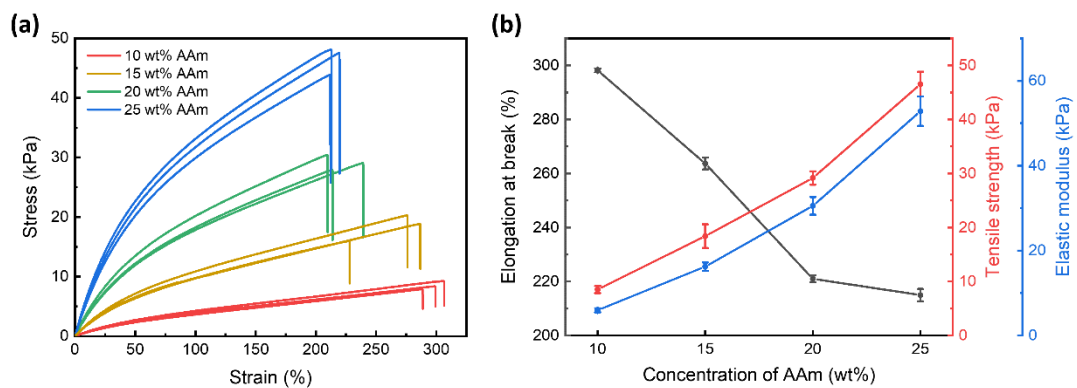


Fig. S7 Mechanical properties of hydrogels. (a) Stress-strain curves and (b) elongation at the break, tensile strength, and the elastic modulus of hydrogels with different concentrations of AAm. All data are shown as mean \pm s.d. of three independent samples.

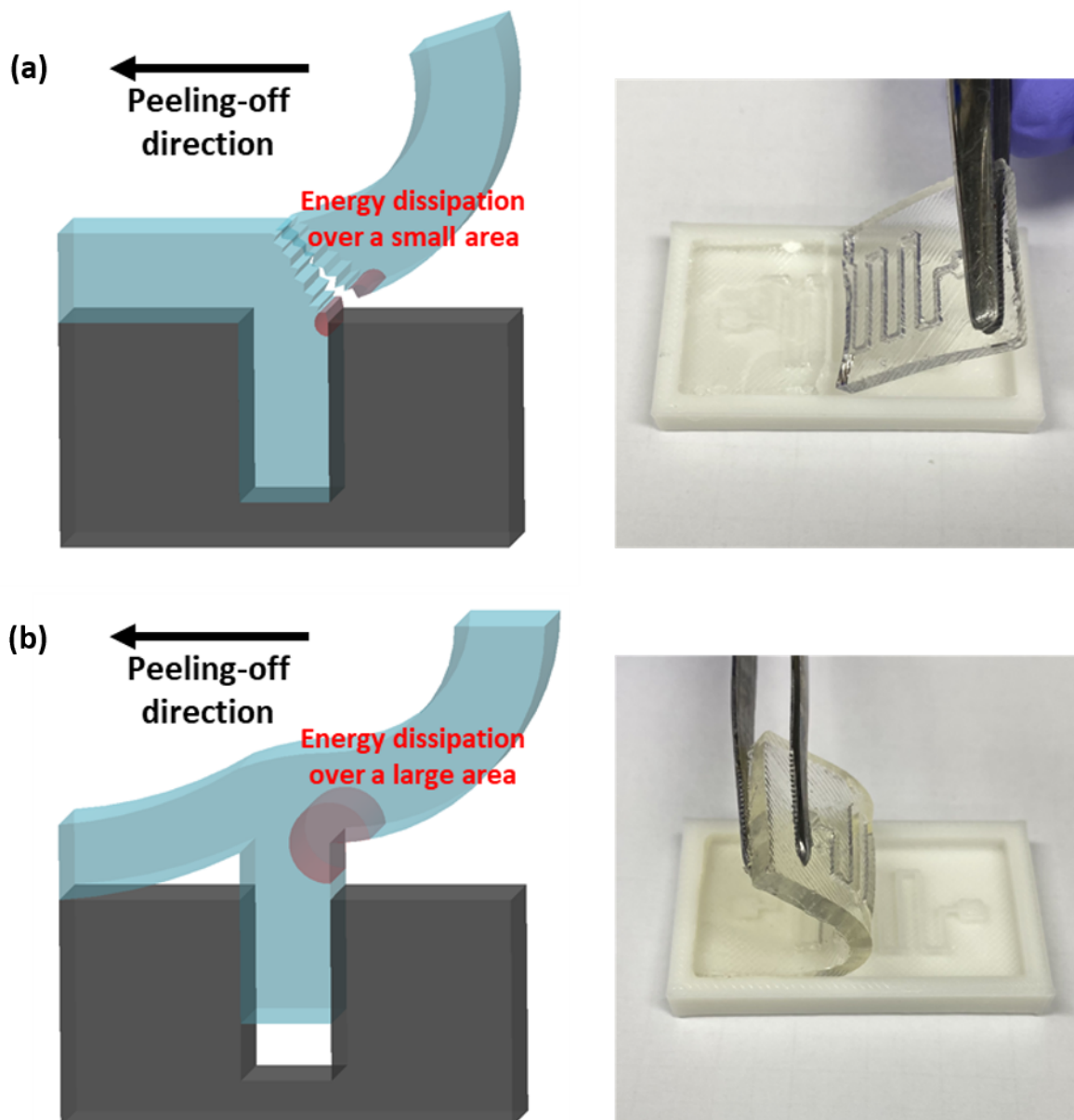


Fig. S8 Schematic illustration of energy dissipation and actual images during the peeling-off process in (a) a rigid hydrogel and (b) a stretchable hydrogel.

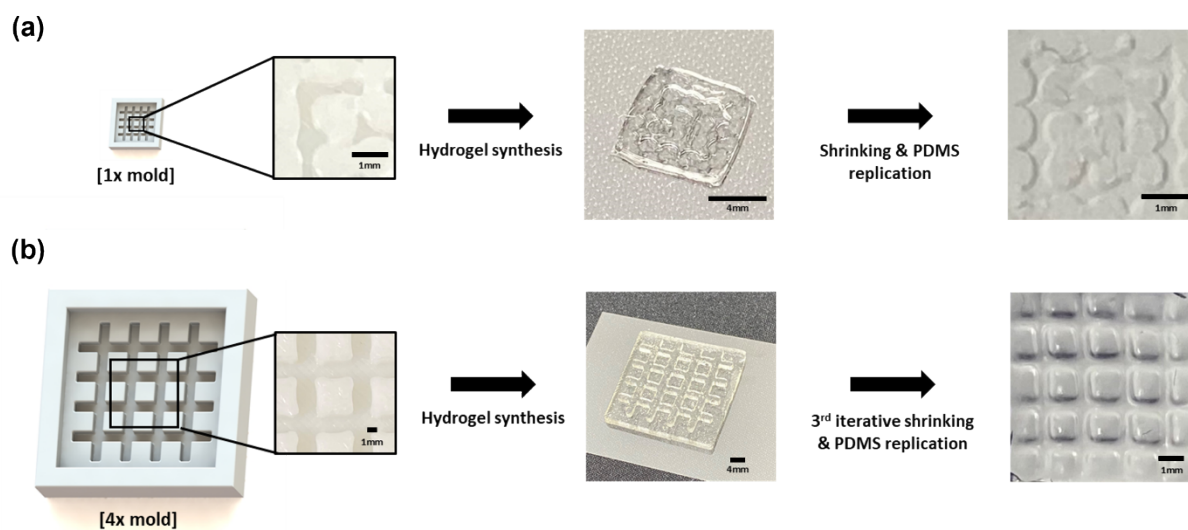


Fig. S9 Molds designed to intersect the four horizontal and vertical lines were fabricated in (a) onefold and (b) fourfold sizes. The structures were compared after shrinkage.

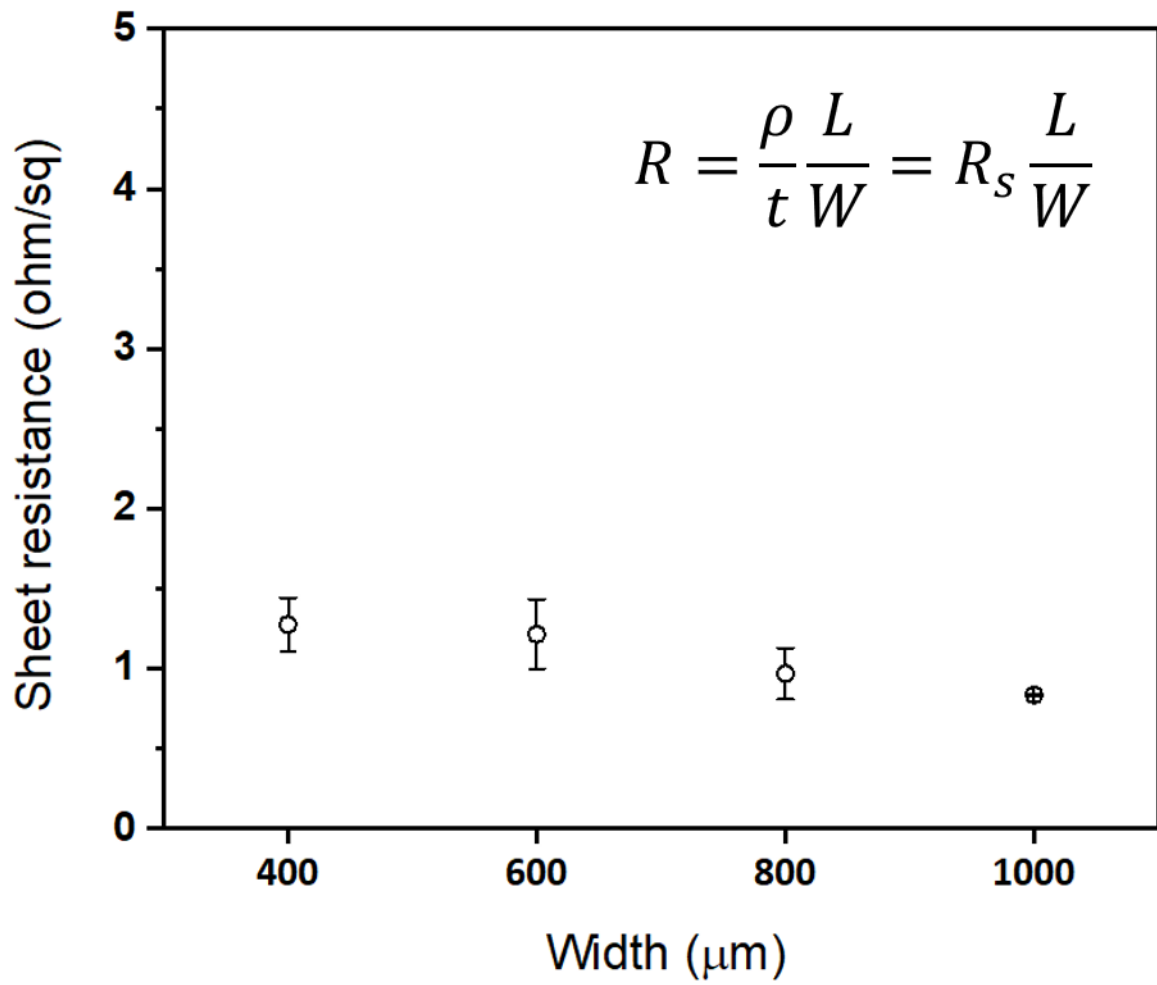


Fig. S10 Sheet resistance as a function of the thickness of the deposited silver nanowire (AgNW) lines.

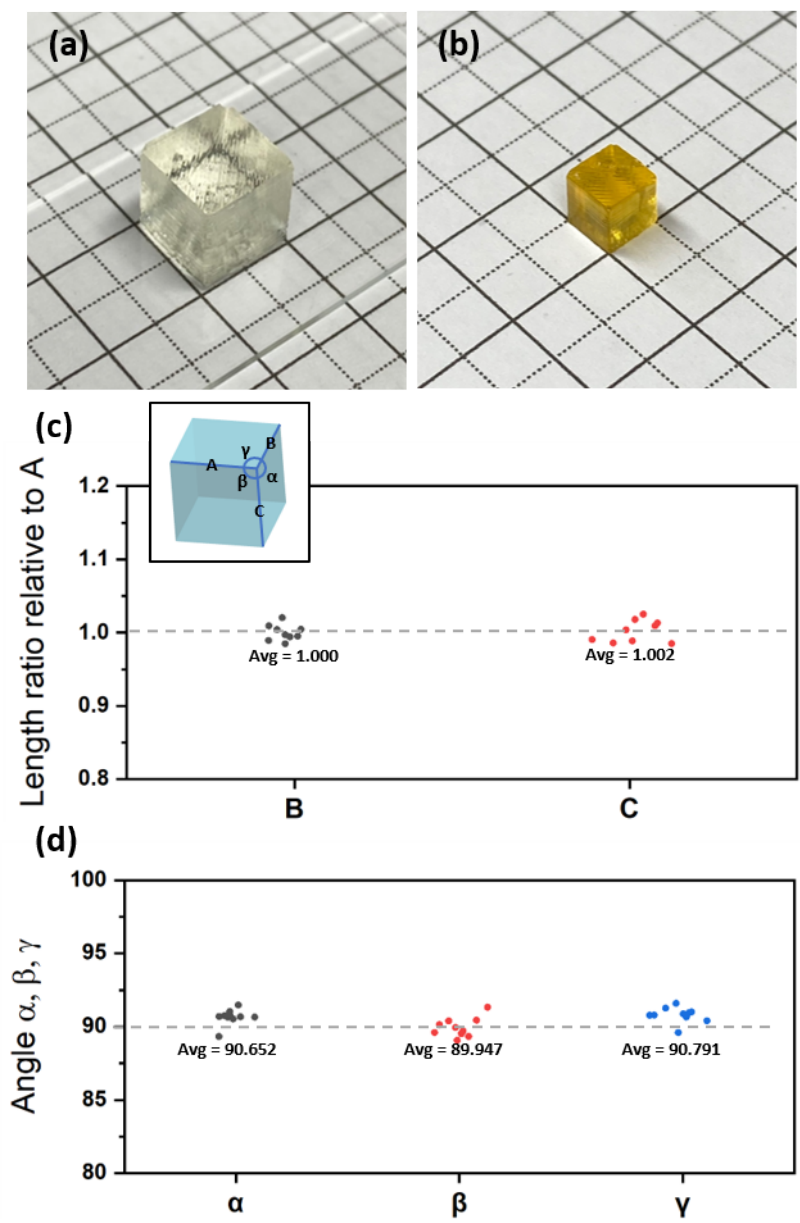


Fig. S11 Images of the cube-shaped hydrogel after (a) synthesis and (b) shrinking for 3D distortion test. (c) The ratios between the adjacent side lengths and (d) the angle degrees of the cube after shrinkage are shown.

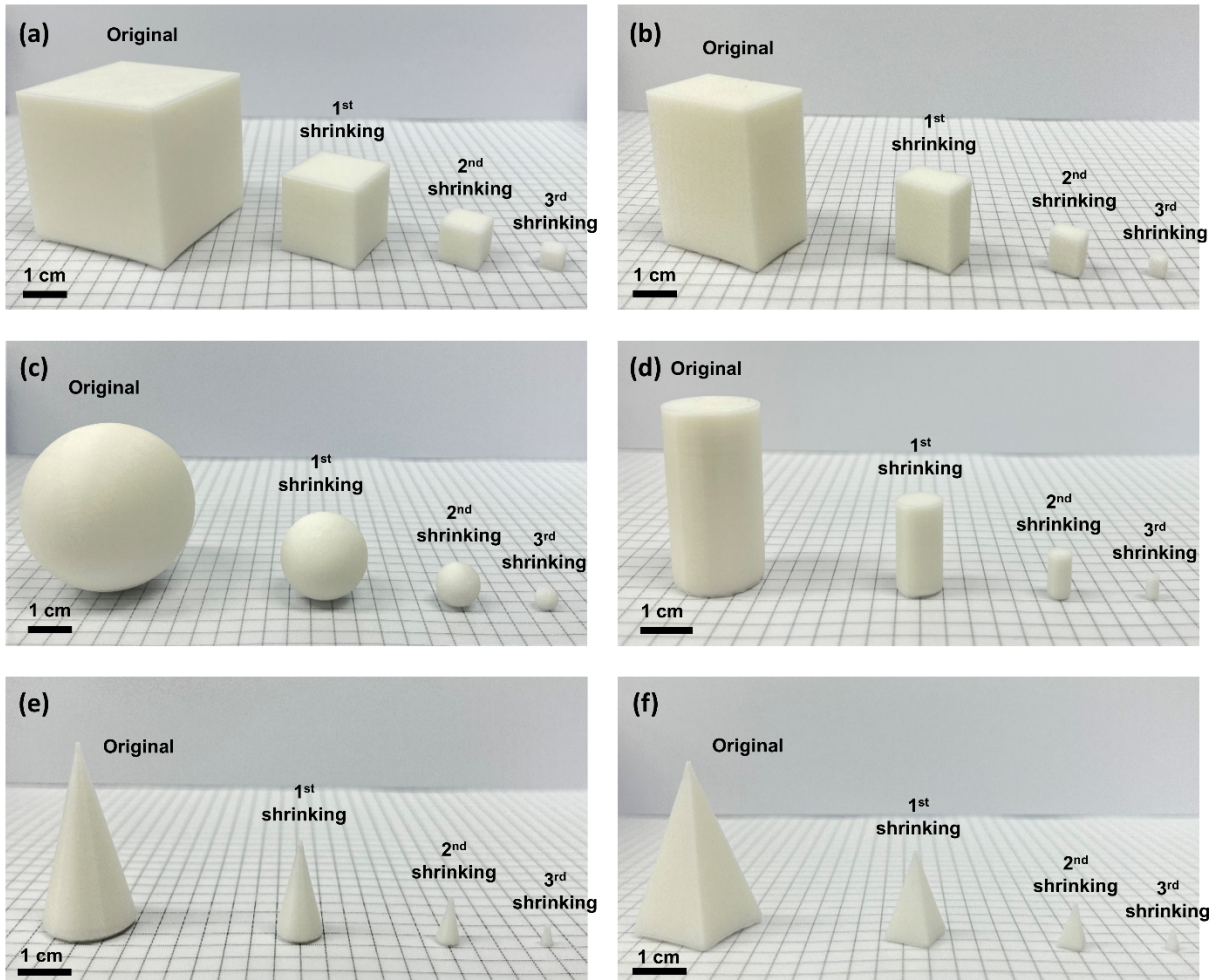


Fig. S12 Images of basic 3D shapes after multiple rounds of shrinkage: (a) cube, (b) cuboid, (c) sphere, (d) cylinder, (e) cone, and (f) pyramid.

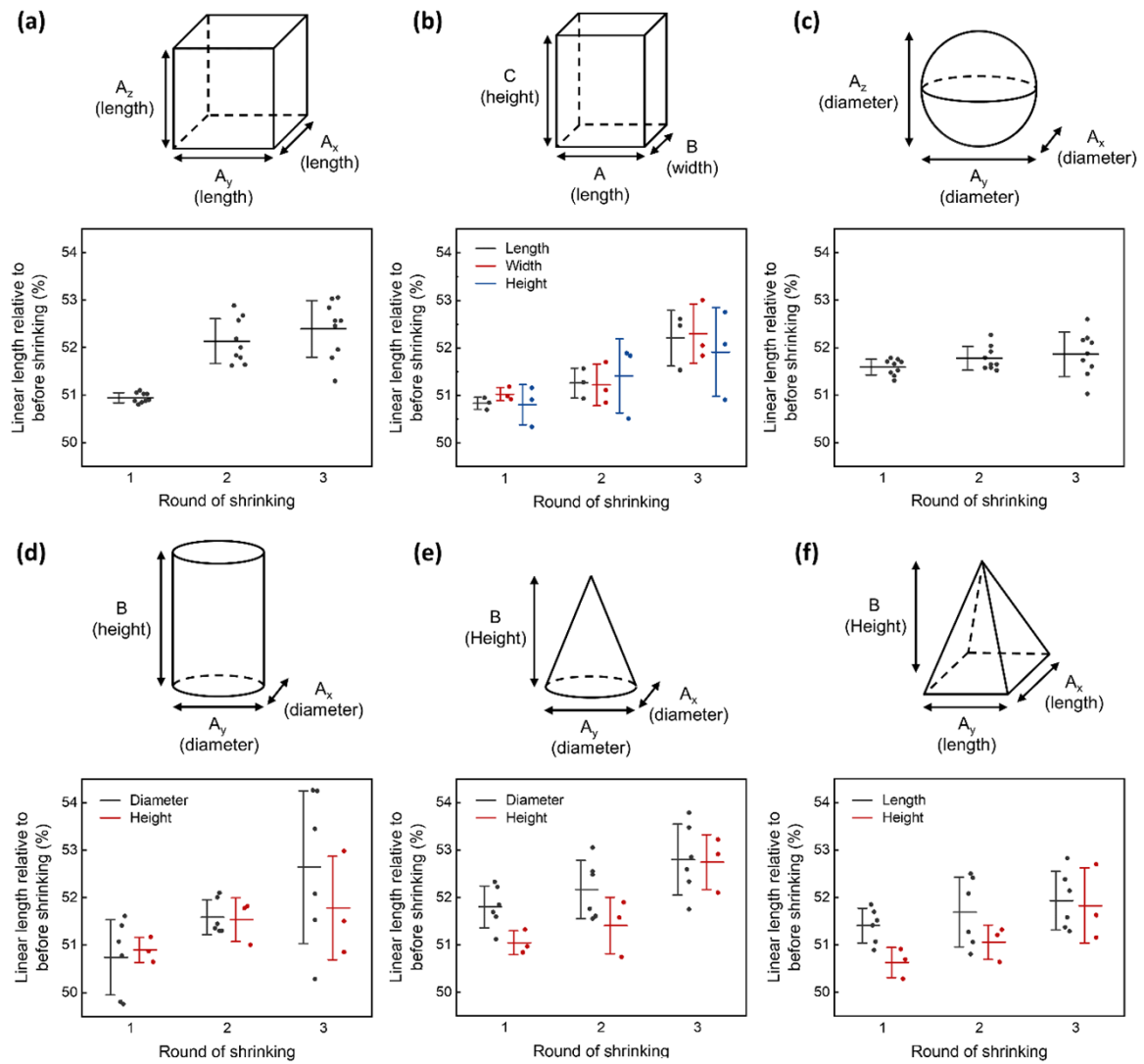


Fig. S13 Degrees of linear shrinkage of 3D basic shapes after multiple rounds of shrinkage: (a) cube, (b) cuboid, (c) sphere, (d) cylinder, (e) cone, and (f) pyramid. All data are shown as mean \pm s.d. of three independent samples.

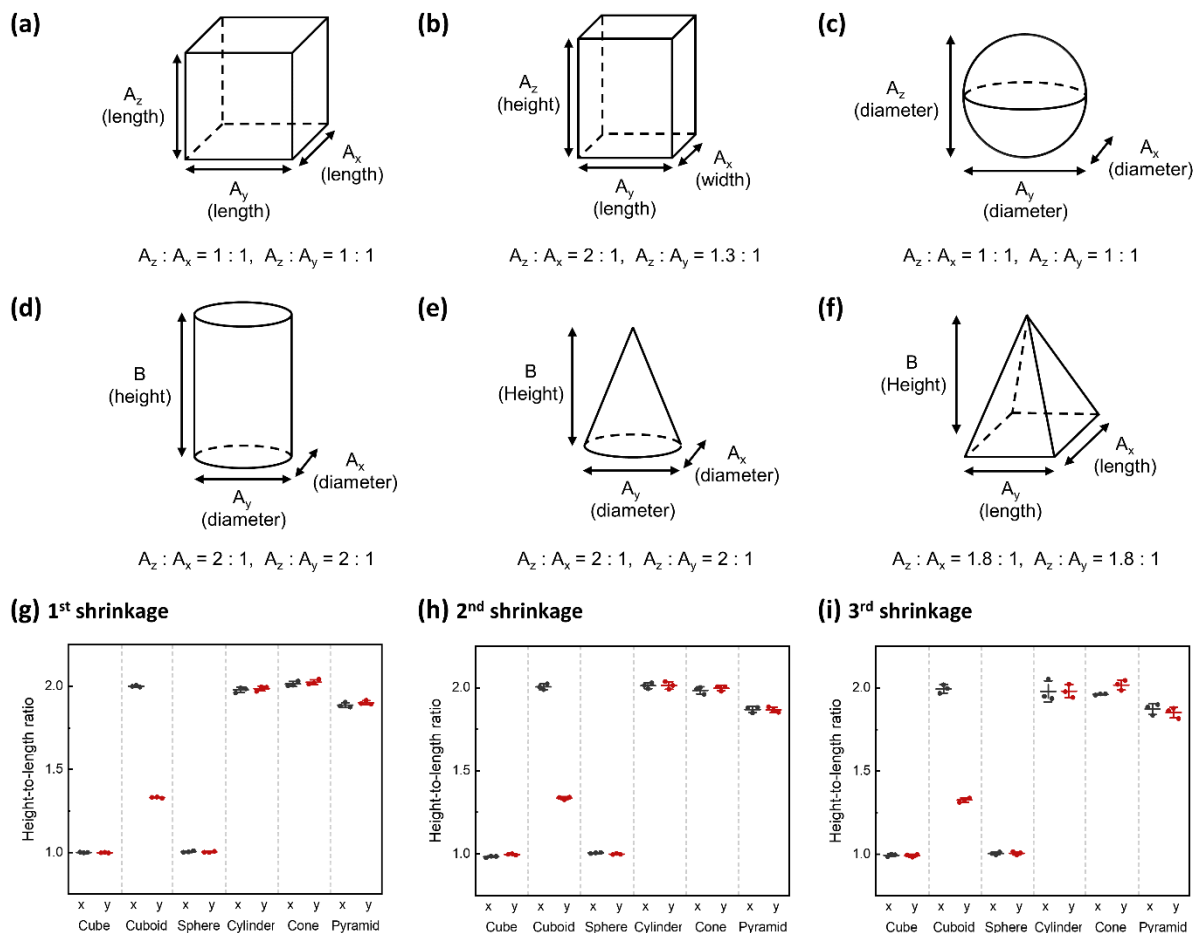


Fig. S14 Linear dimension proportions of 3D basic shapes: (a) cube, (b) cuboid, (c) sphere, (d) cylinder, (e) cone, and (f) pyramid. The height-to-length ratio of each shape after (a) the first shrinkage, (b) the second shrinkage, and (c) the third shrinkage. All data are shown as mean \pm s.d. of three independent samples.

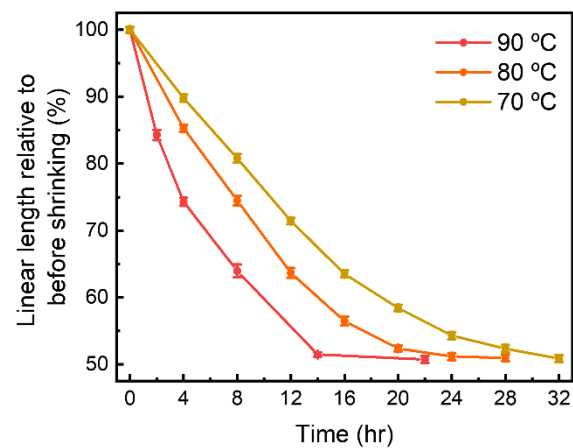


Fig. S15 Shrinking ratio of hydrogels as a function of time at various temperatures. All data are shown as mean \pm s.d. of three independent samples.

Table S1. Composition of hydrogels used to analyze the correlation between the AAm concentration and the shrinkage ratio.

	AAm_5%	AAm_10%	AAm_15%	AAm_20%	AAm_25%
	[wt%]	[wt%]	[wt%]	[wt%]	[wt%]
AAm	5	10	15	20	25
Alginate	2	2	2	2	2
DHEBA	0.06	0.06	0.06	0.06	0.06
APS	0.2	0.2	0.2	0.2	0.2
TEMED	0.2	0.2	0.2	0.2	0.2

Table S2. Shrinkage ratio depending on the acrylamide monomer concentration.

	AAm_5%		AAm_10%		AAm_15%		AAm_20%		AAm_25%	
	D	Relative	D	Relative	D	Relative	D	Relative	D	Relative
	[mm]	percentage	[mm]	percentage	[mm]	percentage	[mm]	percentage	[mm]	percentage
	^{a)}	^{b)}								
		[%]		[%]		[%]		[%]		[%]
Before	7.00	100	7.00	100	7.00	100	7.00	100	7.00	100
1	2.77	39.6	3.16	45.1	3.53	50.4	3.83	54.7	4.16	59.4
2	2.75	39.3	3.11	44.4	3.59	51.3	3.85	55.0	4.12	58.9
3	2.67	38.1	3.10	44.3	3.57	51.0	3.82	54.6	4.16	59.4
4	2.64	37.7	3.14	44.9	3.59	51.3	3.84	54.9	4.15	59.3
5	2.73	39.0	3.09	44.1	3.54	50.6	3.85	55.0	4.14	59.1
6	2.62	37.4	3.16	45.1	3.58	51.1	3.87	55.3	4.14	59.1
7	2.69	38.4	3.12	44.6	3.58	51.1	3.85	55.0	4.15	59.3
8	2.66	38.0	3.20	45.7	3.57	51.0	3.87	55.3	4.14	59.1
9	2.69	38.4	3.09	44.1	3.56	50.9	3.83	54.7	4.19	59.9
average	2.69	38.4	3.13	44.7	3.57	51.0	3.85	54.9	4.15	59.3

^{a)} Diameter of the cylindrical hydrogel; ^{b)} Ratio of the diameter after shrinkage to the diameter before shrinkage.